Investigation of Terahertz Generation due to Unidirectional Diffusion of Carriers in Centrosymmetric GaTe Crystals

Guibao Xu, Guan Sun, Yujie J. Ding, *Senior Member, IEEE*, Ioulia B. Zotova, Krishna C. Mandal, Alket Mertiri, Gary Pabst, Ronald Roy, and Nils C. Fernelius, *Senior Member, IEEE*

***Abstract*—Terahertz (THz) radiation generated by ultrafast laser pulses focused on each monoclinic semiconductor crystal, i.e., GaTe, exhibits unique features. By systemically measuring the dependence of the THz output on the ultrafast pump pulses, in terms of polarization, azimuth angle, incident angle, pump beam size, and pump intensity, we have observed the strong evidence of the unidirectional diffusion of photogenerated carriers within the surface layer of each crystal. Regardless of whether each crystal is pumped above or below its bandgap, the mechanism for THz generation is always attributed to diffusion of the photogenerated carriers. By analyzing data and introducing simplified models, it appears to us that the diffusion of the photogenerated carriers takes place along three different directions.**

***Index Terms*—Broadband terahertz (THz) pulses, centrosymmetric crystal, GaTe, unidirectional diffusion of photogenerated carriers.**

I. Introduction

FOR Terahertz (THz) waves generated in semiconductors by using ultrafast laser pulses, there are primarily two competing mechanisms: optical rectification [1], [2] and photocurrent surge [3], [4]. Both of these two mechanisms have been playing dominant roles in the generation of broadband THz pulses. However, in periodically poled ferroelectric crystals [5], THz pulses having narrow linewidths can be generated based on optical rectification [6]. It is important to note that all the binary compounds studied for THz generation in the past, such as InAs, GaAs, InP, ZnTe, GaP, GaSe, and InN, possess second-order nonlinearities. Therefore, when the photon energy of the pump beam is below the bandgap of each compound, optical rectification usually plays the dominant role for THz generation, whereas above the bandgap either photocurrent surge or combination of the two mechanisms plays a dominant role [7]–[9]. To the best of our knowledge, there has been no report on the THz generation from any centrosymmetric binary-compound semiconductor, which has no second-order nonlinearity.

III–VI chalcogenide semiconductor has a layer-stacking structure with each layer consisting of four monoatomic sheets in the sequence of anion–cation–cation–anion. It exhibits high anisotropy in terms of optical and electrical properties along intralayer and interlayer directions. In particular, GaTe belongs to point group $C2/m$, which has a monoclinic structure. Two-thirds of Ga–Ga dimers are oriented perpendicular to the layers, whereas the remaining one-third of Ga–Ga dimers are almost parallel to the layers. Such a structure is similar to that for GaSe. However, unlike GaSe, GaTe is centrosymmetric, and therefore, its second-order nonlinearity completely vanishes. In contrast, GaSe crystals possess large second-order nonlinear coefficients, and therefore, they have been used for efficient THz generation and sensitive detection based on the large second-order nonlinear coefficients [10]–[12].

Optical and electrical properties of GaTe have been studied for decades [13]–[16], due to its potential applications in detection of radiation at room temperature, optoelectronic devices, thermal energy conversion devices, and bistable switching devices.

In this paper, we demonstrate that GaTe is a promising material for efficient THz emission. We report our results on THz generation from several GaTe crystals doped with Ge, Bi, and Pb at different levels. The highest output powers were measured to be 1.9 μW and 73 nW, corresponding to the pump photon energies of above and below the bandgap of the crystals, respectively. By measuring the dependence of the THz output on polarization, azimuth angle, and incident angle of pump ultrafast pulses, we have observed evidences on unidirectional diffusion of photogenerated carriers, which is dictated by the asymmetry of the crystal structure.

II. Crystal Preparation and Experiment Description

A. Crystal Growth and Preparation

Each undoped GaTe crystal was initially synthesized by melting mixture of high-purity constituent elements with

Manuscript received January 22, 2010; revised March 9, 2010; accepted March 19, 2010. Date of publication April 29, 2010; date of current version February 4, 2011. This work was supported in part by the U.S. Air Force Research Laboratory and in part by the Air Force under Contract FA 86540-06-M-541.

G. Xu, G. Sun, and Y. J. Ding are with the Department of Electrical and Computer Engineering, Center for Optical Technologies, Lehigh University, Bethlehem, PA 18015 USA (e-mail: gux206@lehigh.edu; gus208@lehigh.edu; yud2@lehigh.edu).

I. B. Zotova is with ArkLight, Center Valley, PA 18034 USA (e-mail: yzotova@hotmail.com).

K. C. Mandal is with the Department of Electrical Engineering, University of South Carolina, Columbia SC 29208 USA (e-mail: mandalk@cec.sc.edu).

A. Mertiri is with the Department of Material Science and Engineering, Boston University, Brookline, MA 02446 USA.

G. Pabst and R. Roy are with the EIC Laboratory, Inc., Norwood, MA 02062 USA.

N. C. Fernelius is with the Air Force Research Laboratory, Wright-Patterson Air Force Base, OH 54533 USA and also with Wright State University, Dayton, OH 44435 USA (e-mail: nils.fernelius@wpafb.af.mil).

Color versions of one or more of the figures in this paper are available online at http://ieeexplore.ieee.org.

Digital Object Identifier 10.1109/JSTQE.2010.2046628

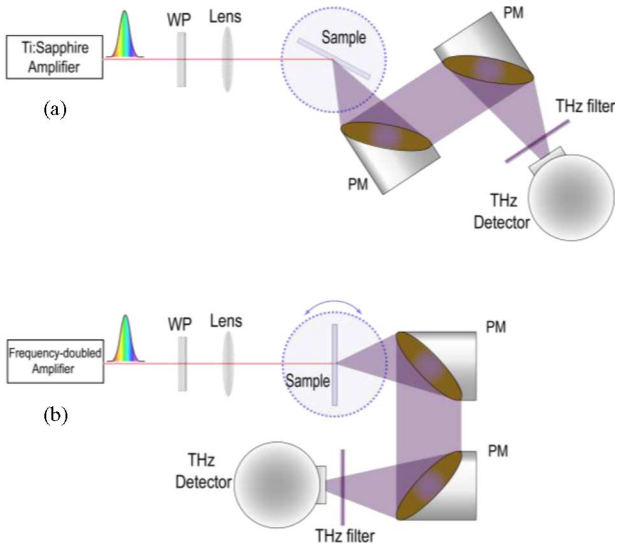

Fig. 1. Experimental setups used in the investigation of THz generation from GaTe crystals. (a) Reflection geometry. (b) Transmission geometry, corresponding to excitation wavelengths of 782 and 391 nm, respectively. WP: half-wave plate; PM: off-axis parabolic mirror. THz filters were used to block the residual pump laser beams while allowing the transmission of the THz waves.

stoichiometric ratio. The obtained ingot was placed in a conically tipped quartz ampoule with appropriate high-purity dopant elements, which was evacuated and sealed off at the pressure of 10^{-6} torr. The ampoule was then heated by a two-zone horizontal furnace, with its temperature being kept as a constant within less than 0.5 °C/cm, in order to introduce different dopants into each GaTe crystal. The details of the crystal growth can be found in [17]. Powder X-ray diffraction confirmed that the grown GaTe crystals had a monoclinic structure with the lattice parameters $a \approx 17.404$ Å, $b \approx 4.077$ Å, and $c \approx 10.456$ Å. Due to the unique layer structure of each GaTe crystal, it can be easily cleaved along the (100) plane to obtain the optics-grade surface.

B. Experiment

Broadband THz pulses were generated by using either a Ti:sapphire regenerative amplifier at 782 nm below the bandgap of the GaTe crystals or a frequency-doubled regenerative amplifier at 391 nm above the bandgap of the crystals. For both the amplifiers, the pulse duration is ~180 fs and repetition rate is set to 250 kHz. When each of the excitation beams was focused onto each GaTe crystal, the THz radiation was collimated, and then, focused onto a 4.2-K Si bolometer or pyroelectric detector by a pair of gold-coated parabolic mirrors in transmission and reflection geometries corresponding to the pump wavelengths of 391 and 782 nm, respectively (see Fig. 1). The Si bolometer was calibrated by using a keating meter. Its response curve is rather flat within the THz region. On the other hand, the pyroelectric detector was calibrated by using the Si bolometer. The responsivity of the pyroelectric detector did not change significantly with the wavelength in the THz region.

TABLE I
SUMMARY MEASUREMENTS ON GaTe CRYSTAL

Crystal ID	Dopant (ppm)	Highest THz Output Power	
		P1* (μW)	P2† (μW)
GTGB8601	Ge/Bi (50/50)	1.422	0.068
GTGP8901	Ge/Pb (50/50)	1.474	0.066
GTG8403	Ge (600)	1.863	0.029
GTG8101	Ge (3000)	1.645	0.073
GTG8112	Ge (4000)	1.789	0.037

Excitation wavelengths: *–391 nm; †–782 nm.

III. RESULTS AND DISCUSSIONS

In this section, we summarize our results of the measurements on a series of GaTe crystals.

A. THz Spectra and Power Dependence

At an average power of 352 mW of the excitation beam at 391 nm, the highest average THz output powers were well above 1 μW for all five samples (see Table I). To the best of our knowledge, this is the first observation of THz emission from a monoclinic centrosymmetric crystal. When these GaTe crystals were excited by the amplifier beam at 782 nm, the highest average THz output powers were approximately 20 times lower.

As we mentioned earlier, there are two competing mechanisms for THz generation in semiconductor materials. Since GaTe has a vanishing second-order nonlinear coefficient due to its centrosymmetric structure, the mechanism for THz generation in GaTe crystals is expected to be photocurrent surge. In such a case, the THz output power increases by increasing the density of photogenerated carriers.An undoped GaTe crystal has the bandgap of about 1.7 eV at room temperature, corresponding to the wavelength of 729 nm. When GaTe was excited below its bandgap, free electrons and holes can be generated by donor–acceptor pair absorption located at 1.57 eV (790 nm) [18], followed by ionization of bound electrons and bound holes by a surface electric field. The diffusion of free photogenerated electrons and holes with different mobilities results in the generation of THz pulses. However, when GaTe was pumped above its bandgap by the frequency-doubled amplifier beam at 391 nm, band-to-band absorption is much higher than the donor–acceptor pair absorption. Therefore, the free-carrier densities generated by the amplifier beam at 782 nm were significantly lower than those generated by the excitation beam at 391 nm. This is the primary reason why the THz output powers generated by the 782-nm beam are much lower.

According to our measurements, the THz output power was increased, as the doping concentration of Ge was significantly increased below 600 ppm. However, above 600 ppm, it was slightly decreased, as the doping concentration was increased further (see Table I). Among all the crystals having different dopants or doping concentrations, the highest output power was measured to be 1.863 μW on the GTG8403 sample with the doping level of 600 ppm at the excitation wavelength of 391 nm. Since the undoped GaTe crystals are p-type, introducing Ge dopants can reduce the free-hole density. As a result, the mobility of the GaTe crystal is increased. Due to Einstein's relation,

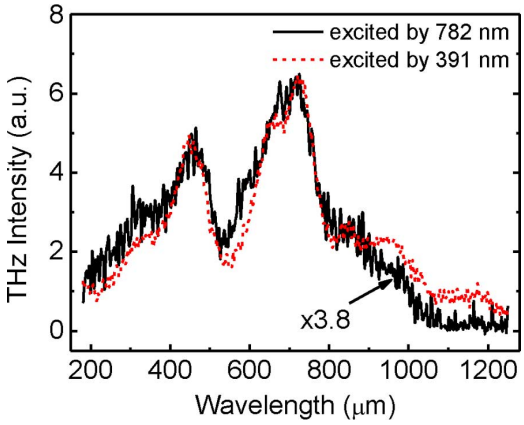

Fig. 2. Typical spectra of THz waves emitted by a GaTe Crystal. Solid and dashed curves correspond to the spectra by using ultrafast laser pulses at 782 and 391 nm as the pump beams, at the pump intensities of 250 and 194 W/cm^2, respectively. The spectral intensities are normalized at the peak wavelength of 720 μm (0.417 THz) for making comparison.

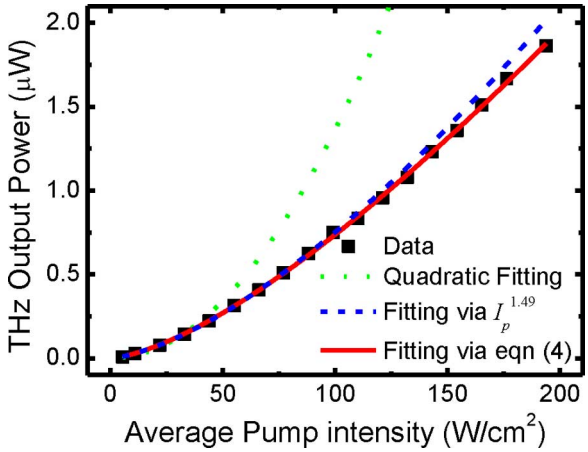

Fig. 3. Average THz output power from GaTe crystal (GTG8403) was measured as a function of average pump intensity. The excitation wavelength was 391 nm. Squares correspond to data. Solid curve corresponds to the nonlinear least-square fitting to all data points by using (4). Dotted curve and dashed curve correspond to the least-square fitting to four and nine data points from the low-intensity end by using quadratic and exponent, respectively.

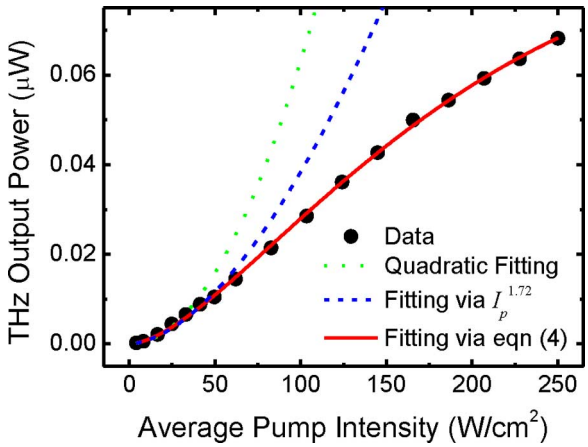

Fig. 4. Average THz output power of GaTe crystal (GTGB8601) was measured as a function of average pump intensity. The excitation wavelength was 782 nm. Circles correspond to data. Solid curve corresponds to the nonlinear least-square fitting to all data points by using (4). Dotted and dashed curves correspond to the least-square fitting to four and seven data points from the low-intensity end by using quadratic and exponent, respectively.

the increase in the mobility leads to the increase in the diffusion constant. Therefore, the THz output power is expected to increase accordingly. Since the THz output powers generated at the excitation wavelength of 782 nm were measured under a large incident angle in the reflection geometry, not all the emitted THz powers were collected. This is the reason why the dependence of the output power on the Ge concentration at 782 nm is not consistent with those at 391 nm.

The spectra of the THz output power for the GaTe crystals were measured by rotating mechanical gratings. From Fig. 2, one can see that THz power spectra cover a frequency range of 240 GHz–1.7 THz, regardless of whether the excitation wavelength is 782 or 391 nm. Based on the high-resolution transmission (HITRAN) molecular absorption database, the pronounced dip located at the wavelength of $\sim$538 μm is attributed to the absorption of water vapor present in the beam path of the THz wave. Based on our measurements, we did not observe any measurable changes of the THz spectra shown by Fig. 2, as the pump intensity was increased. When the GaTe crystal was pumped above its bandgap, the power dependence was well fitted by a square power law for the pump intensities of $\leq$44 W/cm^2. However, it exhibits an increasing deviation from the square power law for the pump intensities of $>$44 W/cm^2 (see Fig. 3). On the other hand, when the GaTe crystal was pumped below its bandgap, the power dependence exhibits stronger saturation, especially for the pump intensities of $>$100 W/cm^2 (see Fig. 4).

Let us assume that the dependence of the THz output power (P_{THz}) on the pump intensity (I_p) and the absorption coefficient for the THz wave (α_{THz}) takes a simple form of [8]

$$P_{\mathrm{THz}} \propto \frac{I_p^2\left[1-\exp(-\alpha_{\mathrm{THz}}L)\right]^2}{\alpha_{\mathrm{THz}}^2} \tag{1}$$

where L is the penetration depth of the pump beam. Due to the generation of the free carriers by the pump laser, a significant fraction of the THz power can be absorbed by the photogenerated carriers. Therefore, the THz absorption coefficient can be approximately written as $\alpha_{\mathrm{THz}} \approx \alpha_0 I_p$, where α_0 is a constant.

As mentioned earlier, photocurrent surge is one of the most plausible mechanisms for the THz generation in the GaTe crystals. In general, the THz emission from a semiconductor surface originates from the drift and/or diffusion current. Since the mobility and kinetic energy of electrons under the optical excitation are much higher than those for holes, the amplitude of THz radiation (E_{THz}) is approximately proportional to the electron mobility $\mu_e(T)$

$$E_{\mathrm{THz}} \propto \frac{\partial J_n}{\partial t} \propto \mu_e(T) \tag{2}$$

where $\mu_e(T)$ varies with the lattice temperature. Generally, it is proportional to T^{-m}, where m is a constant describing a power index. Moreover, during the process of laser pulse excitation on optoelectronic materials, the peak surface temperature is directly proportional to the pulse energy [19]. If we neglect

the energy loss through photoluminescence and assume that all nonradiative transitions end up with the lattice heating, the electron mobility is in the form of

$$\mu_e(T) \propto T^{-m} \propto I_p^{-m}. \tag{3}$$

Under such an assumption, (1) can be reduced to

$$P_{\mathrm{THz}} = C_0 \frac{I_p^{2-n}\left[1-\exp(-\alpha_{\mathrm{THz}}L)\right]^2}{\alpha_{\mathrm{THz}}^2} \tag{4}$$

where C_0 is a constant and $n = 2m$. Let us use (4) as our simplified model to fit the data presented in Figs. 3 and 4, respectively. One can see from Figs. 3 and 4 that we have obtained a perfect agreement between our simplified model described by (4) and our data. One can see that the power index determined from fitting the data is significantly higher for the crystal pumped at 782 nm. This is consistent with our assumption that free carriers were generated by donor–acceptor-pair absorption, followed by ionization of bound electrons and holes. It is worth noting that the penetration depths in a GaTe crystal at the excitation wavelengths of 391 and 782 nm are approximately 40 nm and 65 μm, respectively, due to dramatically different absorption coefficients [20]. Following the nonlinear least-squares fitting, we have obtained the value of $\alpha_0 L$ to be 0.58 and 5.34 cm^2/kW, and the value of n to be 0.51 and 0.28 for the excitation wavelength of 391 and 782 nm, respectively. The ratio between the two values of $\alpha_0 L$ at two different wavelengths reflects the compensation between the large difference in the penetration depths and the densities of the photogenerated carriers generated by the pump beams at 391 and 782 nm. This is due to the fact that α_0 strongly depends on the pump wavelength. Based on our calculation, if the pump intensity is much lower than $(\alpha_0 L)^{-1} \approx 1.72$ kW/cm^2 and 187 W/cm^2 for 391 and 782 nm, respectively, the THz output power versus the pump intensity is perfectly described by a power law with two different indexes (see dashed curves in Figs. 3 and 4). However, when the pump intensity is close to one of the two values given earlier, the power dependence starts to deviate from the power law. Such predicted behaviors are consistent with our data illustrated by Figs. 3 and 4, respectively.

On the other hand, when the pump intensity is sufficiently low, the absorption of the THz wave by the photogenerated carriers becomes negligible. Therefore, (4) can be reduced to $P_{\mathrm{THz}} \propto I_p^2 L$, i.e., the THz output power increases quadratically when increasing the pump intensity. Under such a pumping condition, the strength of the THz electric field is proportional to the time derivative of the diffusion current [see (2)]. Consequently, it can be readily shown that when the density of the photogenerated carriers is sufficiently low, the THz electric field is linearly proportional to the carrier density [21]. Since the carrier density is proportional to the pump intensity, the THz output power is proportional to the square of the pump intensity. Such a simple explanation is consistent with our experimental result under sufficiently low pump intensities (see Figs. 3 and 4).

According to our theoretical model described by (4), the maximum THz power generated by the GaTe crystal is expected to be 29.17 μW at 4.00 kW/cm^2 and 0.090 μW at 0.580 kW/cm^2 at the pump wavelengths of 391 and 782 nm, respectively. Due to the strong saturation of the THz output power as the pump intensity is increased, even under the pump intensity of 2.00 kW/cm^2 at 391 nm, the THz output power has already reached 24.0 μW, which is 82% of the maximum value.

B. Polarization and Azimuth Angle Dependence

As discussed earlier, photocurrent surge is likely the dominant mechanism for the THz generation in the GaTe crystals. Though, it is worth noting that optical rectification could be still one of the possible mechanisms for THz generation, since a surface hexagonal layer can be induced by lattice reorganization in GaTe [23], [24]. One of the characteristics for distinguishing between photocurrent surge and optical rectification for THz generation is the polarization dependence [7].

When GaTe is pumped above its bandgap, the THz output power and polarization angle were measured in the transmission geometry at normal incidence. On the other hand, for the GaTe crystal pumped below its bandgap, our measurement was made in the reflection geometry at an incident angle of 67° for the pump beam. In our measurement, both of the pump intensities were kept constants. The polarization angle of the pump beam ϕ, which is varied by a half-wave plate, is defined as the angle of the pump polarization formed with the incident plane (p-plane), whereas the polarization angle of the THz output beam β, which is monitored by a wire-grid polarizer, is defined as the angle of the THz polarization formed with the same plane. From Figs. 5 and 6, we can see that the THz output power periodically oscillates as a function of the pump polarization. Moreover, the period of the oscillation is the same at the pump wavelengths of 391 and 782 nm. After taking into consideration Fresnel reflections at the crystal/air interfaces, our data can be well fitted by the respective theoretical curves (see the solid curves in Figs. 5 and 6). To obtain the theoretical curve in Fig. 5, we used the refractive indexes of $n_y \approx 4.7988$ and $n_z \approx 3.4862$, which were taken from [20]. At both of the pump wavelengths, the THz polarizations were kept as constants over the entire range of the pump-polarization angles. Such behaviors clearly indicate that photocurrent surge is the primary mechanism for the THz generation in all the GaTe crystals.

Furthermore, since the THz polarization is parallel to the direction of drift or diffusion current, only the photocurrent surge within the crystal surface contributes to the THz output in the transmission geometry under normal incidence. The surface normal of each GaTe crystal is parallel to the $\langle 1\,0\,0\rangle$ direction. According to our fitting result in Fig. 5, the direction for the photocurrent surge within the surface is perpendicular to the $\langle 0\,1\,0\rangle$ direction. This is quite different from the THz wave generated at a typical semiconductor surface due to either drift or diffusion of the photogenerated carriers. In general, for both of the processes mentioned earlier, the directions for the photocurrent surge are typically along the surface normal under normal incidence.

In order to further verify the direction of the photocurrent surge within the crystal surface, the dependences of the THz output power and polarization angle on the azimuth angle were measured on all GaTe crystals using the same setup as that

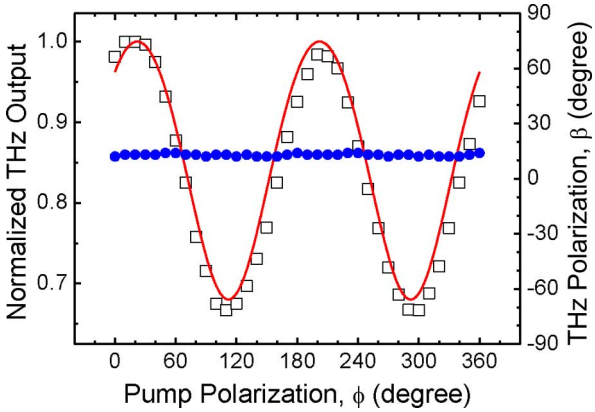

Fig. 5. Measurement of polarization dependence of GaTe crystal (GTGB8601) at the excitation wavelength of 391 nm in transmission geometry. Dots correspond to measured polarization angle of THz beam versus pump polarization. Open squares correspond to normalized average THz output power as a function of pump polarization. Solid curve is theoretical result after taking Fresnel reflections at crystal surface into consideration.

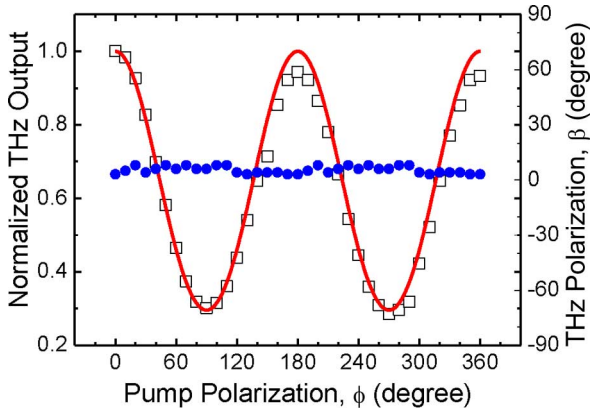

Fig. 6. Measurement of polarization dependence of GaTe crystal (GTGB8601) at the excitation wavelength of 782 nm in reflection geometry. Dots correspond to measured polarization angle of THz beam versus pump polarization. Open squares correspond to normalized average THz output power as a function of pump polarization. Solid curve is theoretical result after taking Fresnel reflections at crystal surface into consideration.

for obtaining Fig. 5 [see Fig. 1(b)]. While the pump beam is p-polarized, each GaTe crystal is rotated around the $\langle 1\,0\,0\rangle$ direction [see Fig. 1(b)]. The azimuth angle of 0° implies that the $\langle 0\,1\,0\rangle$ direction forms 30° with the s-plane. After taking the Fresnel reflections into consideration, our data are fitted by the theoretical curve (see Fig. 7). The visible deviations are caused by spatial inhomogeneity of the GaTe crystal. On the other hand, the THz polarization linearly increases by increasing the azimuth angle through the crystal rotation mentioned earlier. Such a linear dependence confirms our predication that the direction of the photocurrent surge within the crystal surface is perpendicular to the $\langle 0\,1\,0\rangle$ direction.

It is worth noting that the major component of the THz polarization in the measurement made earlier is perpendicular to the $\langle 0\,1\,0\rangle$ direction, whereas the minor component is parallel to the $\langle 0\,1\,0\rangle$ direction within the surface. The ratio between the major and minor components was measured to be about 34.7.

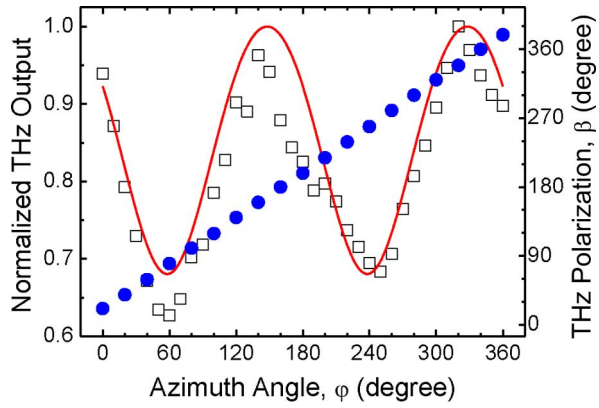

Fig. 7. Azimuth angle dependence of GaTe crystal (GTGB8601). Dots and open squares correspond to measured polarization angle and normalized average THz output power of THz beam, respectively, as a function of the azimuth angle of crystal. Solid curve corresponds to theoretical result after taking Fresnel reflections at crystal surface into consideration.

C. Incident Angle Dependence

Previously, photocurrent surge originated from the drift of the photogenerated carriers under a surface electric field and photo-Dember effect. In order to find out how these two processes affect the THz generation in our crystals, the dependence of the THz characteristics on incident angle was measured on the GaTe crystals. The incident angle θ is defined as the angle of the surface normal formed with the propagation direction of the pump beam. The generated THz output was collected along the direction of the pump propagation. The pump beam at the wavelength of 391 nm was p-polarized during our measurement. In order to minimize the thermal effect, the pump intensity on the crystal surface was kept at $\sim$110 W/cm^2 at normal incidence. The GaTe crystals were rotated around the $\langle 0\,1\,0\rangle$ direction, which is perpendicular to the plane of incidence.

The THz polarizations induced by the drift of the photogenerated carriers and diffusion current originating from photo-Dember effect are shown in inset of Fig. 8. Since the surface field is always along the surface normal, the THz polarization induced by the drift current ($E_\perp$) is along the surface normal, whereas the THz polarization induced by diffusion current (E_D) is along the propagation direction of pump beam inside the GaTe crystal. $E_{/\!/}$ presents the THz polarization induced by the photocurrent surge within the crystal surface, as discussed earlier. The angle of refraction θ_i can be expressed by

$$\theta_i = \arcsin\left[\left(\frac{n_z^2}{\sin^2\theta} - \frac{n_z^2}{n_x^2} + 1\right)^{-1/2}\right] \tag{5}$$

where $n_x = 4.3586$ and $n_z = 3.4862$, as taken from [20]. Based on Fresnel relations at the crystal/air surface, the fraction of the transmitted pulse energy of the pump beam takes the form of

$$S(\theta) = \frac{n(\theta_i)\cos\theta_i}{\cos\theta}\left(\frac{2\cos\theta}{n(\theta_i)\cos\theta + \cos\theta_i}\right)^2 \tag{6}$$

where $n(\theta_i)$ is the refractive index of GaTe.

If we assume that the ratio (A_0) between the contribution of photocurrent surge within the surface and the contribution

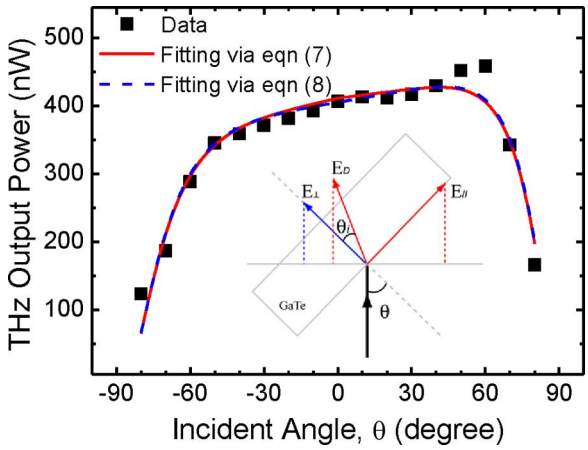

Fig. 8. Average THz output power was measured as a function of incident angle on GaTe crystal (GTGP8901). Squares correspond to data. Solid and dashed curves correspond to nonlinear least-square fitting by using (7) and (8), respectively. Inset illustrates possible THz polarizations induced by different surge currents.

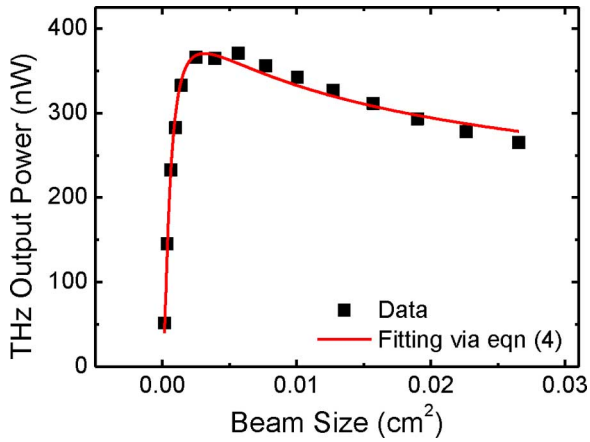

Fig. 9. Average THz output power of GaTe crystal (GTG8101) was measured as a function of beam size of pump wave. Squares and solid curve correspond to data and nonlinear least-square fitting to data by using (4), respectively.

of photocurrent surge perpendicular to the surface is kept as a constant over the entire range of the incident angles, the THz output powers can be determined by the following:

$$P'_{\mathrm{THz}} = C_0[A_0 S(\theta)^2 \cos\theta + S(\theta)^2 \sin(\theta - \theta_i)] \quad (7)$$

and

$$P''_{\mathrm{THz}} = C_0[A_0 S(\theta)^2 \cos\theta + S(\theta)^2 \sin(\theta)] \quad (8)$$

for the combination of E_D and $E_{//}$ and the combination of $E_\perp$ and $E_{//}$, respectively, where C_0 is a constant. One can see from Fig. 8 that our experimental data can be well fitted by using either (7) or (8). The photo-Dember effect is usually caused by the difference in diffusion coefficients for electrons and holes [21]. As discussed in [22], however, such an effect can also be induced by a structural asymmetry. The asymmetry of our data and fitting results relative to the incident angle of 0° implies that the photocurrent surge within the surface is unidirectional, i.e., the photocurrent surge primarily occurs in a direction being perpendicular to the $\langle 0\,1\,0\rangle$ direction within the surface of the crystal. We believe that the THz generation induced by this photocurrent surge is the manifestation of the unidirectional diffusion of the photogenerated carriers. Such a peculiar process was caused by the high degree of anisotropy in the GaTe crystal, which can be attributed to its high degree of the structural asymmetry. To the best of our knowledge, we believe that this is the first report on the evidence of the unidirectional diffusion of the photogenerated carriers within the crystal surface, thus resulting in the efficient THz generation.

Due to the high value of the refractive index for GaTe, even at the incident angle of 80°, the angle of the refracted beam is just ∼16°. Such a small difference between the angles for the drift and diffusion currents is rather difficult to be confirmed in our measurement. On the other hand, if we assume that all the pump photons are converted to the photogenerated carriers, the density of the photogenerated carriers in our experiment reaches $\sim 2.0 \times 10^{20}$ cm^{-3}. Such a value is much larger than that of the typical carrier density due to the surface accumulation. Therefore, we believe that the THz generation from the GaTe crystals is dominated by the diffusion current, i.e., photo-Dember effect.

According to our fitting result shown in Fig. 8 by using (7), the value of ratio A_0 is about 11.1. It is worth noting that in the fitting result by using (8), the value of ratio A_0 is slightly changed to 11.2. The insignificant change of A_0 is consistent with our analysis made earlier. The ratio of the photocurrent surge contributions for the THz generation from the GaTe crystal along the $\langle 0\,1\,0\rangle$ direction within the surface, the direction being perpendicular to the $\langle 0\,1\,0\rangle$ direction within the surface, and the propagation direction of the pump beam inside the crystal is determined to be 1.0 : 34.7 : 3.1.

D. Pump Beam Size Dependence

In order to obtain the optimal pump beam size, we measured the dependence of the THz output power on the beam size of the pump wave at the excitation wavelength of 391 nm. The experimental setup is essentially the same as that used in the measurement of the polarization dependence made earlier [see Fig. 1(b)]. The beam size of the pump wave on the crystal surface was varied by moving a convex lens that was used to focus the pump beam onto the crystal. To avoid the optical damage of the GaTe crystal, the pump power was kept at a constant level of 200 mW. From Fig. 9, one can see that our data can be well fitted by using (4). According to our theoretical model, the optimal pump beam size at the pump power of 200 mW is 3.14×10^{-3} cm^2, which corresponds to a beam waist of ∼447 μm for a Gaussian beam. The corresponding THz output power is 371 nW. When the beam size is decreased to 1.71×10^{-4} cm^2, which corresponds to a beam waist of ∼104 μm for the Gaussian beam, the corresponding THz output power is dramatically reduced to 37 nW, which is only 10% of the maximum output power due to the significant laser heating effect of the GaTe crystal. As the beam size was increased, the laser heating had a much less effect on the THz output power.

IV. Conclusion

In conclusion, we carefully investigated THz generation from centrosymmetric GaTe crystals. Based on our results, the THz generation from the GaTe crystals is primarily induced by the photocurrent surge originating from photo-Dember effect when the crystal is pumped either above or below its bandgap. For the first time to the best of our knowledge, we observed an evidence for the unidirectional diffusion of photogenerated carriers within the crystal surface. The ratio of the photocurrent-surge contributions to the THz generation from the GaTe crystal along the $\langle 0\,1\,0\rangle$ direction within the crystal surface, the direction being perpendicular to $\langle 0\,1\,0\rangle$ within the surface, and the propagation direction of the pump beam inside the crystal is $1.0:34.7:3.1$. Though, we would like to note that further studies must be carried out in the future in order to firmly confirm the unidirectional diffusion of the photogenerated carriers as the primary mechanism for the efficient THz generation in the GaTe crystals. Based on our theoretical model, the maximum THz power generated from the GaTe crystal is 29.17 μW at the pump intensity of 4.00 kW/cm^2 when it is pumped above its bandgap. Due to the unique characteristics for the unidirectional diffusion of the photogenerated carriers within the crystal surface, GaTe is a promising material for scaling up the output power when an external electric field is applied.

References

[1] M. Bass, P. A. Franken, J. F. Ward, and G. Weinreich, "Optical rectification," *Phys. Rev. Lett.*, vol. 9, no. 11, pp. 446–448, Dec. 1962.

[2] K. H. Yang, P. L. Richards, and Y. R. Shen, "Generation of far-infrared radiation by picoseconds light pulses in $LiNBO_3$," *Appl. Phys. Lett.*, vol. 19, no. 9, pp. 320–323, Nov. 1971.

[3] G. A. Mourou, C. V. Stancampiano, A. Antonetti, and A. Orszag, "Picosecond microwave pulses generated with a subpicosecond laser driven semiconductor switch," *Appl. Phys. Lett.*, vol. 39, no. 4, pp. 295–296, Aug. 1981.

[4] A. Leitenstorfer, S. Hunsche, J. Shah, M. C. Nuss, and W. H. Knox, "Femtosecond high-field transport in compound semiconductors," *Phys. Rev. Lett.*, vol. 82, no. 25, pp. 5140–5142, Jun. 1999.

[5] Y. J. Ding and J. B. Khurgin, "A new scheme for efficient generation of coherent and incoherent submillimeter to THz waves in periodically-poled lithium niobate," *Opt. Commun.*, vol. 148, no. 1–3, pp. 105–109, Mar. 1998.

[6] G. Xu, X. Mu, Y. J. Ding, and I. B. Zotova, "Efficient generation of backward terahertz pulses from multiperiod periodically poled lithium niobate," *Opt. Lett.*, vol. 34, no. 7, pp. 995–997, Apr. 2009.

[7] X. Mu, I. B. Zotova, and Y. J. Ding, "Power scaling on efficient generation of ultrafast terahertz pulses," *IEEE J. Sel. Topics Quantum Electron.*, vol. 14, no. 2, pp. 315–332, Apr. 2008.

[8] G. Xu, Y. J. Ding, H. Zhao, G. Liu, M. Jamil, N. Tansu, I. B. Zotova, C. E. Stutz, D. E. Diggs, N. Fernelius, F. K. Hopkins, C. S. Gallinat, G. Koblmüller, and J. S. Speck, "THz generation from InN films due to destructive interference between optical rectification and photocurrent surge," *Semicond. Sci. Technol.*, vol. 25, no. 1, pp. 015004-1–015004-5, Jan. 2010.

[9] X. Mu, Y. J. Ding, and Y. B. Zotova, "Transition from photocurrent surge to resonant optical rectification for terahertz generation in p-InAs," *Opt. Lett.*, vol. 32, no. 22, pp. 3321–3323, Nov. 2007.

[10] W. Shi, Y. J. Ding, N. Fernelius, and K. Vodopyanov, "An efficient, tunable, and coherent 0.18–5.27 THz source based on GaSe crystal," *Opt. Lett.*, vol. 27, no. 16, pp. 1454–1456, Aug. 2002.

[11] K. Liu, J. Xu, and X.-C. Zhang, "GaSe crystals for broadband terahertz wave detection," *Appl. Phys. Lett.*, vol. 85, no. 6, pp. 863–865, Aug. 2004.

[12] C. Kübler, R. Huber, S. Tübel, and A. Leitenstorfer, "Ultrabroadband detection of multi-terahertz field transients with GaSe electro-optic sensors: Approaching the near infrared," *Appl. Phys. Lett.*, vol. 85, no. 16, pp. 3360–3362, Oct. 2004.

[13] W. I. Milne and J. C. Anderson, "Memory switching in gallium telluride single crystals," *J. Phys. D: Appl. Phys.*, vol. 7, no. 11, pp. 1540–1548, Jul. 1974.

[14] S. Pal and D. N. Bose, "Growth, characterization and electrical anisotropy in layered chalcogenides GaTe and InTe," *Solid State Commun.*, vol. 97, no. 8, pp. 725–729, Feb. 1996.

[15] A. A. Al-Ghamdi, "Thermoelectric power (TEP) of layered chalcogenides GaTe crystals," *J. Therm. Anal. Calorimetry*, vol. 94, no. 2, pp. 597–600, Nov. 2008.

[16] A. J. Nelson, A. M. Conway, B. W. Sturm, E. M. Behymer, C. E. Reinhardt, R. J. Nikolic, S. A. Payne, G. Pabst, and K. C. Mandal, "X-ray photoemission analysis of chemically treated GaTe semiconductor surfaces for radiation detector applications," *J. Appl. Phys.*, vol. 106, no. 2, pp. 023717-1–023717-5, Jul. 2009.

[17] K. C. Mandal, S. H. Kang, and M. Choi, "Layered compound semiconductor GaSe and GaTe crystals for THz applications," in *Proc. MRS*, 2007, vol. 969, pp. 111–116.

[18] Y. Cui, D. D. Caudel, P. Bhattacharya, A. Burger, K. C. Mandal, D. Johnstone, and S. A. Payne, "Deep levels in GaTe and GaTe:In crystals investigated by deep-level transient spectroscopy and photoluminescence," *J. Appl. Phys.*, vol. 105, no. 5, pp. 053709-1–053709-4, Mar. 2009.

[19] J. C. Miller and R. F. Haglund, *Laser Ablation and Desorption*. San Diego, CA: Academic, 1998, pp. 175–187.

[20] E. D. Palik, *Handbook of Optical Constants of Solids*. San Diego, CA: Academic, 1998, pp. 489–506.

[21] P. Gu, M. Tani, S. Kono, K. Sakai, and X.-C. Zhang, "Study of terahertz radiation from InAs and InSb," *J. Appl. Phys.*, vol. 91, no. 9, pp. 5533–5537, May 2002.

[22] M. B. Johnston, D. M. Whittaker, A. Corchia, A. G. Davies, and E. H. Linfield, "Simulation for terahertz generation at semiconductor surfaces," *Phys. Rev. B*, vol. 65, no. 16, pp. 165301-1–165301-8, 2002.

[23] E. G. Gillan and A. R. Barron, "Chemical vapor deposition of hexagonal gallium selenide and telluride films from cubane precursors: Understanding the envelope of molecular control," *Chem. Mater*, vol. 9, no. 12, pp. 3037–3048, Dec. 1997.

[24] O. A. Balitskii, B. Jaeckel, and W. Jaegermann, "Surface properties of GaTe single crystals," *Phys. Lett. A*, vol. 372, no. 18, pp. 3303–3306, Apr. 2008.

Guibao Xu received the B.E. and Ph.D. degrees from Shandong University, Jinan, China, in 2000 and 2006, respectively.

From 2004 to 2006, he was a Visiting Scholar at Max-Born-Institut, Berlin, Germany and Institut National de Métrologie, Paris, France. Since 2006, he has been a Postdoctoral Fellow and a Research Associate in the Department of Electrical and Computer Engineering, Lehigh University, Bethlehem, PA. He is the author or coauthor of more than 40 refereed journal articles in nonlinear optical effects and devices, two-photon upconversion organic compounds, solid state laser, and Raman scattering in nitride heterostructure and terahertz (THz) generation. His current research interests include THz generation, amplification, detection and application, and nonlinear optical devices.

Guan Sun received the B.S. degree from Fudan University, Shanghai, China in 2008. He is currently working toward the Ph.D. degree in the Department of Electrical and Computer Engineering, Lehigh University, Bethlehem, PA.

His current research interests include terahertz generation, applications, and III–nitride-based LEDs.

Yujie J. Ding (M'04–SM'05) received the B.S. degree from Jilin University, Jilin, China, in 1984, the M.S.E.E. from Purdue University, West Lafayette, IN, in 1987, and the Ph.D. degree from Johns Hopkins University, Baltimore, MD, in 1990.

From 1990 to 1992, he was a Postdoctoral Fellow, and then, an Associate Research Scientist at Johns Hopkins University. During 1992–1999, he was an Assistant and an Associate Professor of physics at Bowling Green State University, Bowling Green, OH. From 1999 to 2002, he was an Associate Professor of physics at the University of Arkansas, Fayetteville. In 2002, he joined Lehigh University, Bethlehem, PA where he is currently a Professor in the Department of Electrical and Computer Engineering. He is the author or coauthor of more than 140 refereed journal articles in optoelectronics, nonlinear optics, and quantum electronics. His research interests include terahertz generation, amplification and detection, nanostructures and nanodevices, Raman scattering in nitride heterostructures, and their applications.

Prof. Ding is a Fellow of the Optical Society of America. He is the recipient of the Class of 1961 Professorship from Lehigh University in 2003 and the Outstanding Young Scholar Award from Bowling Green State University in 1996.

Ioulia B. Zotova received the B.S. degree from the Russian Mendeleev University of Chemical Technology, Moscow, Russia, in 1997, the M.S. degree from Bowling Green State University, Bowling Green, OH, in 1999, and the Ph.D. degree from the University of Arkansas, Fayetteville, in 2002.

Since 2003, she has been at ArkLight, Center Valley, PA. Her current research interests include terahertz devices and spectrometers, detections of biological and chemical agents, and single-photon detections.

Krishna C. Mandal received the M.Sc. degree in chemistry and the Ph.D. degree in materials science from the Indian Institute of Technology (IIT), India, in 1981 and 1988, respectively.

He was the Director of solid-state sensors and detectors in the Advanced Materials Division, EIC Laboratories, Inc., Norwood, MA. He was in the Chemical Physics Group, Tata Institute of Fundamental Research, Mumbai, India, where he was engaged in II–VI semiconductors, and their bulk and thin-film devices. He was a Research Associate at the Condensed Matter Physics Division, Ecole Polytechnique, Paris, France, and then, at the Materials Engineering Department, Ecole Polytechnique, Montreal, QC, Canada. He was an Electronic Materials Scientist at the Noranda Advanced Materials Division, Noranda, QC. He is currently an Associate Professor of electrical engineering at the University of South Carolina, Columbia, SC. His research interests include lightweight and flexible photovoltaic solar cells based on nanocrystalline materials, high-energy physics and radiation detectors, medical imaging devices, mid- to longwave-infrared lasers, and terahertz sources and detectors.

Dr. Mandal is a member of the Electrochemical Society, the American Physical Society, the Materials Research Society, and the Society of Photographic Instrumentation Engineers.

Alket Mertiri received the B.S. degree in physics and mathematics from Boston University, Boston, MA, in 2006, where he is currently working toward the Ph.D. degree in the Department of Material Science and Engineering.

His current research interests include design, fabrication, and characterization of biomicroelectromechanical systems for studying cell response to different combination of stimuli.

Gary Pabst, photograph and biography not available at the time of publication.

Ronald Roy, photograph and biography not available at the time of publication.

Nils C. Fernelius (M'85–SM'00) received the A.B. degree from Harvard University, Cambridge, MA, in 1956, and the M.S. and Ph.D. degrees from the University of Illinois, Urbana-Champaign, in 1959 and 1966, respectively, all in physics.

During 1956–1957, he was at Oxford University, Oxford, U.K. He has been a Research Associate at the University of Illinois, an Assistant Physicist at Argonne National Laboratory, Argonne, IL, a National Research Council Senior Fellow at Wright-Patterson Air Force Base (AFB), Dayton, OH, a Physicist at the University of Dayton Research Institute, Dayton, and a Physicist in the Materials Directorate of the Air Force Research Laboratory, Wright-Patterson AFB. He is currently an Adjunct Associate Professor of physics at Wright State University, Dayton. His research interests include frequency conversion and terahertz devices, systems, and applications.

Dr. Fernelius is a Life Member of American Physical Society, a member of the Optical Society of America, the Society of Photographic Instrumentation Engineers (SPIE), the Materials Research Society, the Society for Applied Spectroscopy, Sigma Xi, and the American Association of Physics Teachers. He was the Chair of the Solid State Laser Committee of Lasers and Electro-Optics Society from 2002 to 2005. He was the recipient of the George Rappaport Award from Society for applied spectroscopy in 1995.